Available online at www.sciencedirect.com
SCIENCE DIRECT®
Journal of Crystal Growth 283 (2005) 141–146
JOURNAL OF CRYSTAL GROWTH
www.elsevier.com/locate/jcrysgro

Nucleation and growth behavior of well-aligned ZnO nanorods on organic substrates in aqueous solutions

Chin-Ching Lin[a], San-Yuan Chen[a,*], Syh-Yuh Cheng[b]

[a]*Department of Materials Science and Engineering, National Chiao Tung University, 1001 Ta-hsueh Rd., Hsinchu, Taiwan*
[b]*Materials Research Laboratories, Industrial Technology Research Institution, Chutung. Taiwan*

Received 1 October 2004; received in revised form 13 May 2005; accepted 20 May 2005
Available online 21 July 2005
Communicted by J.M. Redwing

Abstract

A low-temperature synthetic route was used to prepare well-aligned arrays of oriented ZnO nanorods on organic substrates coated with polystyrene beads (PS) in an aqueous solution. The corresponding growth behavior and photoluminescence properties of ZnO nanorods were analyzed. It was found that the ZnO nanorods are initially nucleated from the ZnO monolayer under the concave regions of the PS layers and preferentially grown along [0 0 0 1] direction. High-resolution transmission electron microscopy (HRTEM) observation reveals that the ZnO nanorods tend to coalesce together with other adjacent nanorods to form a larger ZnO crystal in the later growth stage. The room-temperature photoluminescence spectra demonstrate that a stronger ultraviolet (UV) emission with a broad yellow emission around 575 nm was observed for the ZnO nanorods grown on the organic substrates and the relative intensity ratio of ultraviolet emission to yellow emission depends on the growth periods of time. This simple approach demonstrates great potential for optoelectronic devices because it can produce large-scale highly well-aligned ZnO nanorods on the flexible organic substrates at lower temperatures.

Keywords: A1. Nanostructures; A2. Hydrothermal crystal growth; B1. Zinc compounds

1. Introduction

One-dimensional ZnO nanostructures have been extensively studied for their potential applications in manufacturing electronic and optoelectronic devices [1–3]. The ZnO nanorods have been thought of as the most suitable for ultraviolet (UV) laser devices because of their wide direct band gap of 3.37 eV and a relatively large exciton binding energy of 60 meV [4]. Furthermore, many reports have demonstrated that directionally grown ZnO nanorods can effectively decrease the

*Corresponding author. Tel.: + 886 3 5731818; fax: + 886 3 5725490.
E-mail address: sychen@cc.nctu.edu.tw (S.-Y. Chen).

0022-0248/$ - see front matter © 2005 Elsevier B.V. All rights reserved.
doi:10.1016/j.jcrysgro.2005.05.065

threshold power to achieve the UV lasing emission at room temperature [5–7]. A variety of methods have been employed, including vapor phase transport [6], metal-organic chemical vapor deposition (MOCVD) [7], thermal decomposition [8] and hydrothermal synthesis [9]. However, those are expensive and energy-consuming processes since they are operated under extreme conditions. Recently, many wet-chemical approaches have been developed to prepare oriented arrays of ZnO nanorods on polycrystalline (or single crystalline) substrates from aqueous solutions [10–15]. However, it is worth noting that without suitable treatment on the Si substrate, highly oriented ZnO nanorods have been rarely achieved.

Recently, Choy et al. [16] and Tian et al. [17] used ZnO nanoparticles as seeds to grow the large-scale and well-oriented ZnO nanorods on Si substrates from chemical solutions. However, it is potentially important to synthesize 1D nanoscale materials on organic substrates in the applications of flexible display and photoelectronic devices. Although the growth of ZnO nanowires on a flexible two-inch polydimethylsiloxane substrate has been reported by Greene et al. [18] the substrate with a network of microscale cracks was observed. So far, to the best of our knowledge, there has been no further and systematical investigation on the nucleation and growth behavior of ZnO nanowires grown on organic substrates in an aqueous solution at a lower temperature.

In this work, an organic substrate with polystyrene beads (PS) coated will be used for the growth of well-aligned arrays of oriented ZnO nanorods in aqueous solutions at low temperatures. Both nucleation mechanism and growth behavior of oriented ZnO nanorods will be investigated. In addition, photoluminescence (PL) properties of the ZnO nanorods on the organic substrates are also discussed in this study.

2. Experimental procedure

To grow the ZnO nanorods on organic substrates (polycarbonate, PC), regular polystyrene beads (PS) (diameter around 100 nm) were dissolved in ethanol solvent and then deposited on the substrates following the process proposed by Xia et al. [19]. The PS-coated organic (PC) substrates were then placed in glass bottles containing an equimolar (0.04 M) aqueous solution of $Zn(NO_3)_2 \cdot 6H_2O$ and hexamethylenetetramine (HMT) at 75 °C for different times (0–25 h). After that, the substrates were removed from the aqueous solutions, rinsed with distilled water, and dried at room temperature overnight. Moreover, in order to understand the nucleation of the ZnO nanorods on the organic substrate, the PS beads can be removed by immersing the samples in toluene. The obtained ZnO nanorods were characterized by field-emission scanning electron microscopy (FE-SEM) using JAM-6500F and a transmission electron microscope (TEM) with Philips TECNAI 20. PL of the ZnO nanorods was performed by excitation from a 325 nm He–Cd laser at room temperature. The chemical compositions were examined by X-ray photoelectron spectroscopy (XPS).

3. Results and discussion

Fig. 1(a) shows the surface image of large-scale arrayed ZnO nanorods grown on the polystyrene beads (PS)/polycarbonate (PC) substrates. It was found that the ZnO nanorods have a well-defined hexagonal plane with a homogeneous diameter of approximately ~60 nm due to uniform growth rate. The cross-sectional SEM image in Fig. 1(b) demonstrates that the ZnO nanorods are directionally and densely grown over the entire PS surface of the substrates. Furthermore, it was noted that the well-aligned ZnO nanorods in Fig. 1(c) remained unchanged after the removal of the PS beads from the specimen fabricated using the same conditions as Fig. 1(b). This implies that the PS layer can supply the appropriate environment for the nucleation and growth of ZnO nanorods.

To understand how the well-aligned ZnO nanorods were developed on the organic substrates, the samples were grown at 75 °C for different periods of time. The initial stage ($t < 0.5$ h) can be considered as the induction time

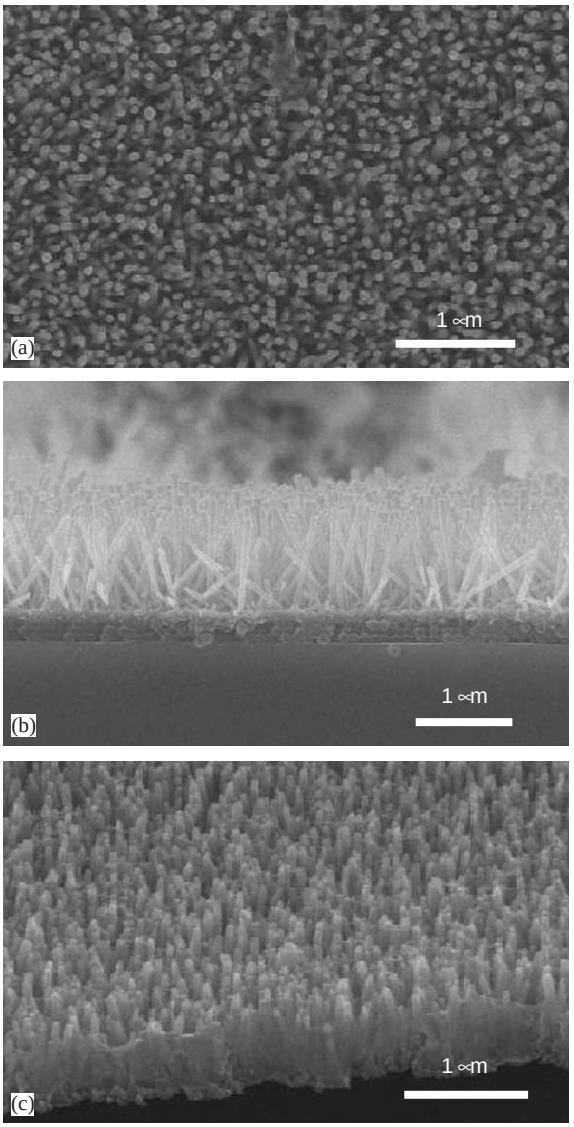

Fig. 1. SEM images of large arrays of oriented ZnO nanorods grown on polystyrene (PS)/polycarbonate (PC) substrates for 8 h. (a) Low magnification, face-on view. (b) Cross-sectional SEM image of ZnO nanorods grown on PS/PC substrates. (c) SEM image of ZnO nanorods grown on PS/PC substrates after removing the PS beads.

during which an ultra-thin monolayer was slowly generated under the PS beads. However, it was difficult to observe the ultra-thin monolayer by SEM, but this layer can be justified to be ZnO by X-ray photon spectroscopy (not shown here) after

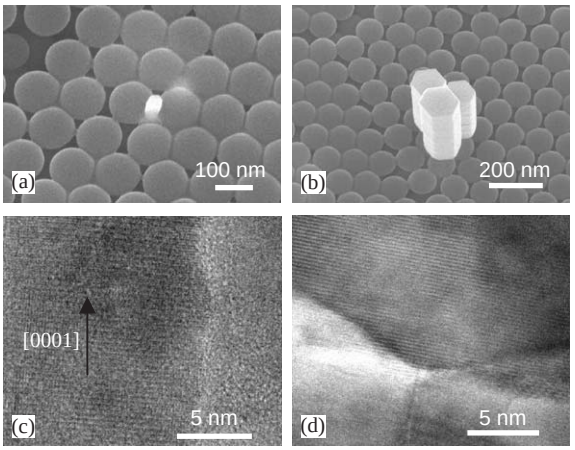

Fig. 2. SEM images of ZnO nanorods grown on PS/PC substrates at 75 °C for (a) 1 h and (b) 5 h. (c) High-resolution TEM image of the ZnO nanorods grown on organic substrate. (d) High-resolution TEM image of the interface region between ZnO nanorods and ultra-thin ZnO monolayer on PC substrate.

removing the PS beads. Later, in the second stage, the ZnO nanorods started to nucleate from the concave regions of the PS layers as evidenced from Fig. 2(a). It was believed that the promotion of heterogeneous nucleation on the concave regions may be ascribed to the high affinity of the ZnO nuclei to the ZnO layer under the PS beads. To investigate the nucleation behavior of the aligned ZnO nanorods, high-resolution TEM (HRTEM) was used to study the interface between ZnO nanorods and ZnO monolayer (~5 nm thicker) after removing the PS beads. Fig. 2(d) illustrates that the ZnO nanorods are preferentially nucleated on the concave region from ZnO monolayer. A similar phenomenon has been observed for the aligned ZnO nanorods grown on the Si substrates buffered with ZnO film [17,20]. After nucleation, in the third stage, a preferential growth along the longitudinal direction (*c*-axis) for the oriented ZnO nanorods was expected because the ZnO growth unit (or coordination polyhedron) will stack in order and grow along [0 0 0 1] direction as observed in Fig. 2(c). The lattice fringes are perpendicular to the longitudinal direction of the ZnO nanorods and the singular fringe spacing is measured about 0.51 nm that is nearly consistent with the *c*-axis parameter in hexagonal ZnO

structure ($c = 0.521$ nm in wurtzite ZnO). A detailed investigation for the growth behavior of ZnO nanorods grown on an inorganic substrate (Si) coated with ZnO film can be referred to our previous study [20]. This demonstrates that the well-aligned ZnO nanorods can be grown on both organic and inorganic substrates at a lower temperature from aqueous solutions. After long-term growth, i.e., 24 h, the SEM surface image of the ZnO nanorods in Fig. 3(a) reveals that the ZnO nanorods have started on a coalescence process with other adjacent nanorods. As compared with Fig. 1(a), the ZnO nanorods become much larger (more than 0.5 μm) in diameter but show little change (about 1.7 μm) in length. The TEM bright-field (BF) image (inset in Fig. 3(a)) of the face-on view ZnO nanorods clearly demonstrates the merged grains with side crystal plane attached that can be further confirmed by the [0 0 0 1] zone-axis selected-area electron diffraction (SAED) pattern of ZnO nanorods as shown in Fig. 3(b). The split diffraction spots in the edge region (marked with arrows) of the SAED pattern can be observed and this suggests that the merged ZnO nanorods are not perfectly aligned in both *a* and *b* directions. Figs. 3(c) and (d) show the TEM BF and dark-field (DF) images of the cross-sectional merged ZnO nanorods, respectively. More than two ZnO nanorods were aggregated in a coplanar manner using their side planes to form a larger ZnO nanorod. A magnified picture of Fig. 3(c) was illustrated in Fig. 3(e) where the SAED pattern of the coalescent nanorods (labeled as 3 in Fig. 3(d)) is also shown in the right inset. This further demonstrates that a slight misalignment could occur during the coalescence of ZnO nanorods. Therefore, the growth behavior of the ZnO nanorods in the later growth stage can be considered as a direct combination of a small number of individual nanorods that was similar to oriented attachment [21].

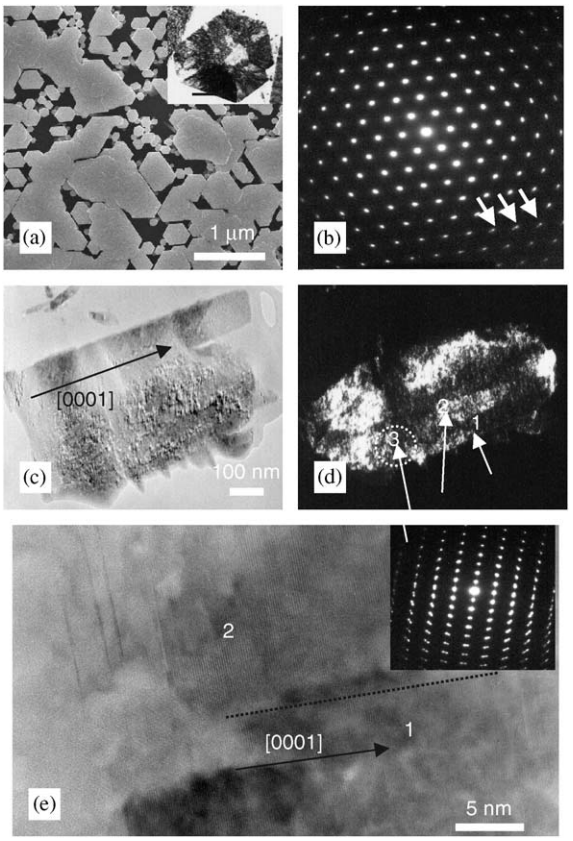

Fig. 3. (a) Face-on view SEM image of well-aligned ZnO nanorods grown on PS/PC substrates for long-term growth (24 h). A [0 0 0 1] zone-axis TEM bright-field (BF) image of the coalescent ZnO nanorods (its scale bar is 100 nm in the inset), and (b) a corresponding diffraction pattern in the inset of Fig. 3(a). (c) Cross-sectional TEM (BF) and (d) dark-field (DF) images of the coalescent ZnO nanorods. (e) A high magnification BF TEM image of Fig. 3(c) shows the interface (marked with dash line) of the coalescent couple ZnO nanorods with the diffraction pattern in the inset.

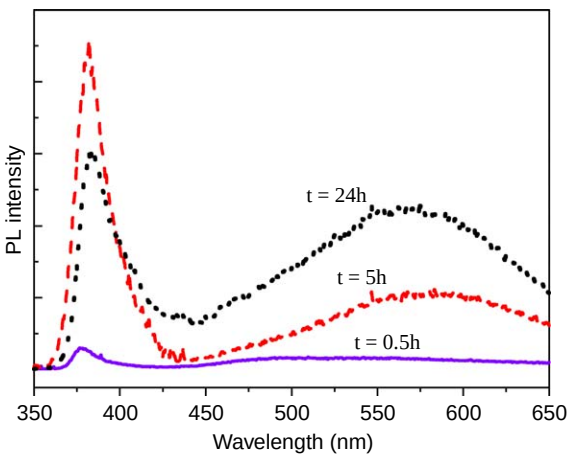

Fig. 4. Room-temperature PL spectra of ZnO nanorods grown on PS/PC substrates for different growth period of time.

Fig. 4 illustrates the room-temperature PL spectra of the ZnO nanorods grown on PS/PC substrates. For ZnO nanorods grown for a short period of time, i.e., 0.5 h, only a weak PL peak around 378 nm is detected, which corresponds to the ultraviolet (UV) emission of ZnO with a bandgap of 3.27 eV. Generally, the UV emission peak of ZnO is attributed to an exciton-related activity [22]. As the ZnO nanorods were grown for 5 h, a strong PL emission at 380 nm, corresponding to the 3.26 eV bandgap transition of ZnO, was detected. However, a broad yellow emission around 570 nm was also observed [23]. Similar observation for ZnO nanorods fabricated by the same chemical method was also reported by Li et al. [24]. The deep level involved in the yellow luminescence is likely interstitial oxygen [24–26]. The relative PL intensity ratio of ultraviolet emission (I_{UV}) to deep level emission (I_{DLE}) is estimated to be about ~5.1. Furthermore, the PL properties are strongly influenced by chemical stoichiometry and microstructure defects of the materials [27]. According to our previous results [20], the ZnO nanorods grown in the aqueous solution at a lower temperature may induce unstable surface status to trap impurities and further damage the optical properties. Especially for the ZnO nanorods with a long-term growth, i.e. 24 h, the broad yellow emission becomes stronger compared to that of ZnO nanorods grown for 5 h. The relative PL ratio (I_{UV}/I_{DLE}) is reduced from 5.1 to 1.2. This may be attributed to the increased native defects because of imperfect boundaries and misalignment between ZnO nanorods for the merged ZnO nanorods. However, the above-mentioned results suggest that both native defects and optical quality of the ZnO nanorods grown on a flexible substrate at low temperatures can be controlled by changing growth conditions.

4. Conclusions

In summary, we have developed a low-temperature synthetic route to grow well-aligned arrays of oriented ZnO nanorods on organic substrates in an aqueous solution. HRTEM analysis demonstrates that the well-aligned ZnO nanorods are preferentially nucleated from the ZnO monolayer under concave regions of PS layers. However, a long-term growth process leads to the formation of a larger ZnO crystal due to coplanar coalescence of several individual ZnO nanorods. In addition, it was observed that the optical quality of the ZnO nanorods could be improved by controlling growth conditions. This simple approach shows great potential for optoelectronic devices because it can produce large-scale highly well-aligned ZnO nanorods on flexible organic substrates.

Acknowledgments

The authors gratefully acknowledge the financial support of the National Science Council of Taiwan in the Republic of China through Contract NSC-92-2216-E-009-014.

References

[1] Y. Cui, C.M. Liber, Science 291 (2001) 851.
[2] W.I. Park, G.–C. Yi, M. Kim, S.J. Pennycook, Adv. Mater. 15 (2003) 526.
[3] X. Duan, Y. Huang, Y. Cui, J. Wang, C.M. Lieber, Nature 409 (2001) 66.
[4] M. Zamirescu, A. Kavokin, B. Gil, G. Malpuech, M. Kaliteevski, Phys. Rev. B 65 (2002) 161205.
[5] M.H. Huang, S. Mao, H. Feick, H. Yan, Y. Wu, H. Kind, E. Weber, R. Russo, P. Yang, Science 292 (2001) 1897.
[6] M.H. Huang, Y. Wu, H. Feick, N. Tran, E. Weber, P. Yang, Adv. Mater. 13 (2001) 113.
[7] W.T. Chiou, W.Y. Wu, J.M. Ting, Diam. Relat. Mater. 12 (10-11) (2003) 1841.
[8] N. Audebrand, J.P. Auffredic, D. Louer, Chem. Mater. 10 (1998) 2450.
[9] C-H. Lu, C-H. Yeh, Ceram. Int. 26 (2000) 351.
[10] L. Guo, J.X. Cheng, X.Y. Li, Y.J. Yan, S.H. Yang, C.L. Yang, J.N. Wang, W.K. Ge, Mater. Sci. Eng. C 16 (2001) 123.
[11] L. Guo, S.H. Yang, C.L. Yang, J.N. Wang, W.K. Ge, Chem. Mater. 12 (2000) 2268.
[12] J. Zhang, L.D. Sun, H.Y. Pan, C.S. Liao, C.H. Yan, New J. Chem. 26 (2002) 33.
[13] L. Vayssieres, Adv. Mater. 15 (2003) 464.
[14] L. Vayssieres, K. Keis, S.–E. Lindquist, A. Hagfeldt, J. Phys. Chem. B 105 (2001) 3350.
[15] L. Vayssieres, K. Keis, A. Hagfeldt, S.–E. Lindquist, Chem. Mater. 13 (12) (2001) 4395.

[16] J.H. Choy, E.S. Jang, J.H. Won, J.H. Chung, D.J. Jang, Y.W. Kim, Adv. Mater. 15 (2003) 1911.
[17] Z.R. Tina, J.A. Voigt, J. Liu, B. Mckenzie, M.J. Mcdermott, M.A. Rodriguez, H. Konishi, H. Xu, Nature Mater. 2 (2003) 821.
[18] L.E. Greene, M. Law, J. Goldberger, F. Kim, J.C. Johnson, Y. Zhang, R.J. Saykall, P. Yang, Angew. Chem. Int. Ed. 42 (2003) 3031.
[19] Y. Xia, Y. Yin, Y. Lu, J. McLellan, Adv. Funct. Mater. 13 (2003) 907.
[20] S.C. Liou, C.S. Hsiao, S.Y. Chen, J. Crystal Growth 274 (2004) 438.
[21] C. Pacholski, A. Kornowski, H. Weller, Angew. Chem. Int. Ed. 41 (2002) 1188.
[22] D.M. Bagnall, Y.F. Chen, Z. Zhu, T. Yao, Appl. Phys. Lett. 70 (1997) 2230.
[23] S.A. Studenikin, N. Golego, M. Cocivera, J. Appl. Phys. 84 (1998) 2287.
[24] D. Li, Y.H. Leung, A.B. Djurisic, Z.T. Liu, M.H. Xie, S.L. Shi, S.J. Xu, W.K. Chan, Appl. Phys. Lett. 85 (2004) 1601.
[25] X.L. Wu, G.G. Siu, C.L. Fu, H.C. Ong, Appl. Phys. Lett. 78 (2001) 2285.
[26] L.E. Greene, M. Law, J. Goldberger, F. Kim, J.C. Johnson, Y. Zhang, R.J. Saykally, P. Yang, Angew. Chem. Int. Ed. 42 (2003) 3031.
[27] A.B. Djurisic, W.C.H. Choy, V.A.L. Roy, Y.H. Leung, C.Y. Kwong, K.W. Cheah, T.K. Gundu Rao, W.K. Chan, H. Fei. Lui, C. Surya, Adv. Funct. Mater. 14 (2004) 856.